Stem Cell Research (2013) 10, 179–194

Available online at www.sciencedirect.com

SciVerse ScienceDirect

www.elsevier.com/locate/scr

Albumin gene targeting in human embryonic stem cells and induced pluripotent stem cells with helper-dependent adenoviral vector to monitor hepatic differentiation

Kahoko Umeda [a, 1], Keiichiro Suzuki [c, 1], Taiji Yamazoe [a, b], Nobuaki Shiraki [a], Yuichiro Higuchi [a], Kumiko Tokieda [a], Kazuhiko Kume [a], Kohnosuke Mitani [c,*], Shoen Kume [a, b,**]

[a] *Department of Stem Cell Biology, Institute of Molecular Embryology and Genetics, Kumamoto University, Honjo 2-2-1, Kumamoto 860-0811, Japan*
[b] *The Global COE, Kumamoto University, Honjo 2-2-1, Kumamoto 860-0811, Japan*
[c] *Gene Therapy Division, Research Center for Genomic Medicine, Saitama Medical University, Hidaka, Saitama 350-1241, Japan*

Received 31 July 2012; received in revised form 10 October 2012; accepted 9 November 2012
Available online 27 November 2012

Abstract Although progresses in developing differentiation procedures have been achieved, it remains challenging to generate hES/iPS cell-derived mature hepatocytes. We performed knock-in of a monomeric Kusabira orange (mKO1) cassette in the *albumin* (*ALB*) gene, in human embryonic stem (hES) cells and induced pluripotent stem (hiPS) cells, with the use of the helper-dependent adenovirus vector (HDAdV). Upon induction into the hepatic lineages, these knock-in hES/iPS cells differentiated into cells that displayed several known hepatic functions. The mKO1 knock-in (*ALB*/mKo1) hES/hiPS cells were used to visualize hepatic differentiation in vitro. mKO1 reporter expression recapitulated endogenous *ALB* transcriptional activity. *ALB*/mKo1 [Hi] population isolated by flow cytometry was confirmed to be enriched with *ALB* mRNA. Expression profile analyses revealed that characteristic hepatocyte genes and genes related to drug metabolism and many aspects of liver function were highly enriched in the *ALB*/mKo1 [Hi] population. Our data demonstrate that *ALB*/mKo1 knock-in hES/iPS cells are valuable resources for monitoring in vitro hepatic differentiation, isolation and analyses of hES and hiPS cells-derived hepatic cells that actively transcribing *ALB*. These knock-in hES/iPS cell lines could provide further insights into the mechanism of hepatic differentiation and molecular signatures of the hepatic cells derived from hES/iPS cells.

Abbreviations: ALB, Albumin; mKO1, monomeric Kusabira orange; hES, human embryonic stem; hiPS, human induced pluripotent stem; HDAdV, Helper-dependent adenovirus; AFP, Alpha-fetoprotein; GO, Gene ontology.

* Corresponding author. Fax: +81 42 984 4655.
** Correspondence to: S. Kume, Department of Stem Cell Biology, Institute of Molecular Embryology and Genetics, Kumamoto University, Honjo 2-2-1, Kumamoto 860-0811, Japan. Fax: +81 96 373 6807.
E-mail addresses: mitani@saitama-med.ac.jp (K. Mitani), skume@kumamoto-u.ac.jp (S. Kume).
[1] Equal contribution.

1873-5061/$ - see front matter © 2012 Elsevier B.V. All rights reserved.
http://dx.doi.org/10.1016/j.scr.2012.11.003

Introduction

The liver plays a central role in multiple functions of the human body including detoxification of drugs and storage of nutrients. Animal models exhibit different metabolic profiles from humans and are thus not directly applicable to humans. Human primary hepatocytes are valuable for assessing drug toxicity and testing drug kinetics (Davila et al., 2004) but these applications are impeded from limited availability and differences between samples. In addition to their use in drug development, hepatocytes are expected to be an alternative therapeutic approach for producing transplantable hepatocytes since severe liver dysfunctions are treatable only by liver transplantation in many cases.

Embryonic stem (ES) cells are derived from the inner cell mass of the fertilized egg, which is pluripotent, and can be cultured indefinitely in an undifferentiated state and have the potential to differentiate into various cell types derived from the three germ layers (Evans and Kaufman, 1981; Kaufman et al., 1983; Suemori et al., 2001; Thomson et al., 1998). Induced pluripotent stem (iPS) cells (Takahashi and Yamanaka, 2006; Takahashi et al., 2007, 2009; Belmonte et al., 2009) resemble ES cells but raise fewer ethical concerns because they can be derived from somatic cells. ES cells and iPS cells represent powerful tools for studying basic developmental biology and are potential sources of hepatocyte generation for applications in regenerative medicine and drug development (Davila et al., 2004).

ES and iPS cells have been shown to recapitulate developmental processes and differentiate into hepatic lineages in vitro following the sequential addition of growth factors. Recently, human ES cells were directed to differentiate in a stepwise manner into the definitive endoderm, hepatic lineages, and hepatocytes following the addition of Activin/Nodal, fibroblast growth factor (FGF), BMP, retinoic acid (RA), Wnt3a and dimethyl sulfoxide (DMSO), hepatocyte growth factor (HGF), and oncostatin M (OSM) (Touboul et al., 2010; Shiraki et al., 2008a, 2008b; Sullivan et al., 2010; Hay et al., 2008a, 2008b; Cai et al., 2007; Zaret and Grompe, 2008; Si et al., 2010; Katsumoto et al., 2010).

We have previously established a procedure in which ES cells are sequentially induced in vitro into the mesendoderm, definitive endoderm, and regional specific digestive organs such as the pancreas and liver (Shiraki et al., 2008a, 2008b, 2009). Approximately 80% of the hES that were cultured on a monolayer of the M15 mesonephric-derived cell line and given growth factors differentiated into α-fetoprotein (AFP)-positive hepatic precursor cells and approximately 10% of cells later became albumin (ALB)-positive cells and secreted a substantial level of ALB protein (Shiraki et al., 2008b). Recently, we found that optimization of the culture condition and culturing cells on a synthesized basement membrane (sBM) resulted in an improvement of ALB secretion (Shiraki et al., 2011).

Modification of endogenous genes by homologous recombination is well established and practiced in mouse ES cells. However, although several reports have described gene targeting by electroporation in hES cells (Zwaka and Thomson, 2003; Urbach et al., 2004; Di et al., 2008; Ruby and Zheng, 2009; Sakurai et al., 2010), the efficiencies of stable transfection (random integration) were extremely low (approximately 1×10^{-6} per cell) and the ratio of targeted to random chromosomal integration was also low (approximately 2%). In contrast, the helper-dependent adenovirus vector (HDAdV) was a reportedly efficient and versatile gene targeting vector in mouse ES cells and allowed the insertion of a long homologous sequence of up to 35 kb (Ohbayashi et al., 2005). HDAdV was originally developed to overcome host immune responses against E1D AdVs in vivo (Palmer and Ng, 2005). Because all of the viral genes are removed from the vector genome, HDAdVs offer additional advantages such as decreased cytotoxicity and expanded cloning capacity, permitting insertion of longer segments of homologous DNA for homologous recombination. These features are advantageous for obtaining highly efficient site-specific integration into host chromosomes through homologous recombination. The HDAdV system was shown to be a powerful tool for genetic manipulation in hES and human iPS (hiPS) cells. When HDAdVs were used to target several loci, the recombination efficiencies were 3–55% (Suzuki et al., 2008; Aizawa et al., 2012). Recently, targeted gene correction in patient-specific iPS cells was reported using HDAdVs (Liu et al., 2011; Li et al., 2011). Taken together, gene transfer mediated by HDAdVs is a powerful technology for genetic manipulation in hES and hiPS, both for biological studies and therapeutic applications.

Herein, to trace the differentiation and analyze human ES or iPS cell-derived hepatocytes, we carried out gene targeting of a reporter transgene to the *ALB* locus and established *ALB*/monomeric Kusabira orange1 (mKO1) knock-in (*ALB*/mKo1) hES and hiPS cell lines, and report here the use of these knock-in hES and hiPS cell lines, cultured under a modified version of our previously established differentiation procedure (Shiraki et al., 2008b).

Material and methods

Construction of the ALB/mKo1 bacterial artificial chromosome (BAC) clone and the pHDAdV *ALB*/mKo1-PGKneo vector

The human BAC clone RP11-281P16 contains the human *ALB* gene locus from the RPCI-11 Human Male BAC Library (Osoegawa et al., 2001) and was purchased from BACPAC Resources. The BAC-based targeting vector was generated by a 2-step recombineering modification (Copeland et al., 2001). First, the zeocin resistance gene (p23-loxP-Zeo) was targeted into the loxP site of the human *ALB* BAC clone RP11-281P16 (BACPAC Resources). The mKO1 reporter cassette, pKS-mKO1-loxP-Neo-loxP, was constructed using mKO1 cDNA from pmKO1-MC1 (Medical & Biological Laboratories) (Karasawa et al., 2004). Homology arms were then inserted on the 5′ and 3′ ends of the cassettes to generate pKS-h*ALB*-Larm-mKO1-loxP-PGK-EM7-Neo-loxP-Rarm. Second targeting; mKO1-PGK-EM7-Neo was then targeted into the ATG site of *ALB* exon 1 of RP11-281P16 to generate BAC-*ALB*/mKo1-loxP-Neo (Supplementary Fig. 1). A 23-kb fragment from the BAC-*ALB*/mKo1-loxP-Neo vector, which included 101,721–124,538 bp of RP11-281P16 and the reporter fragment, was retrieved into pBC-HDAdTKβgal1-PISceI by

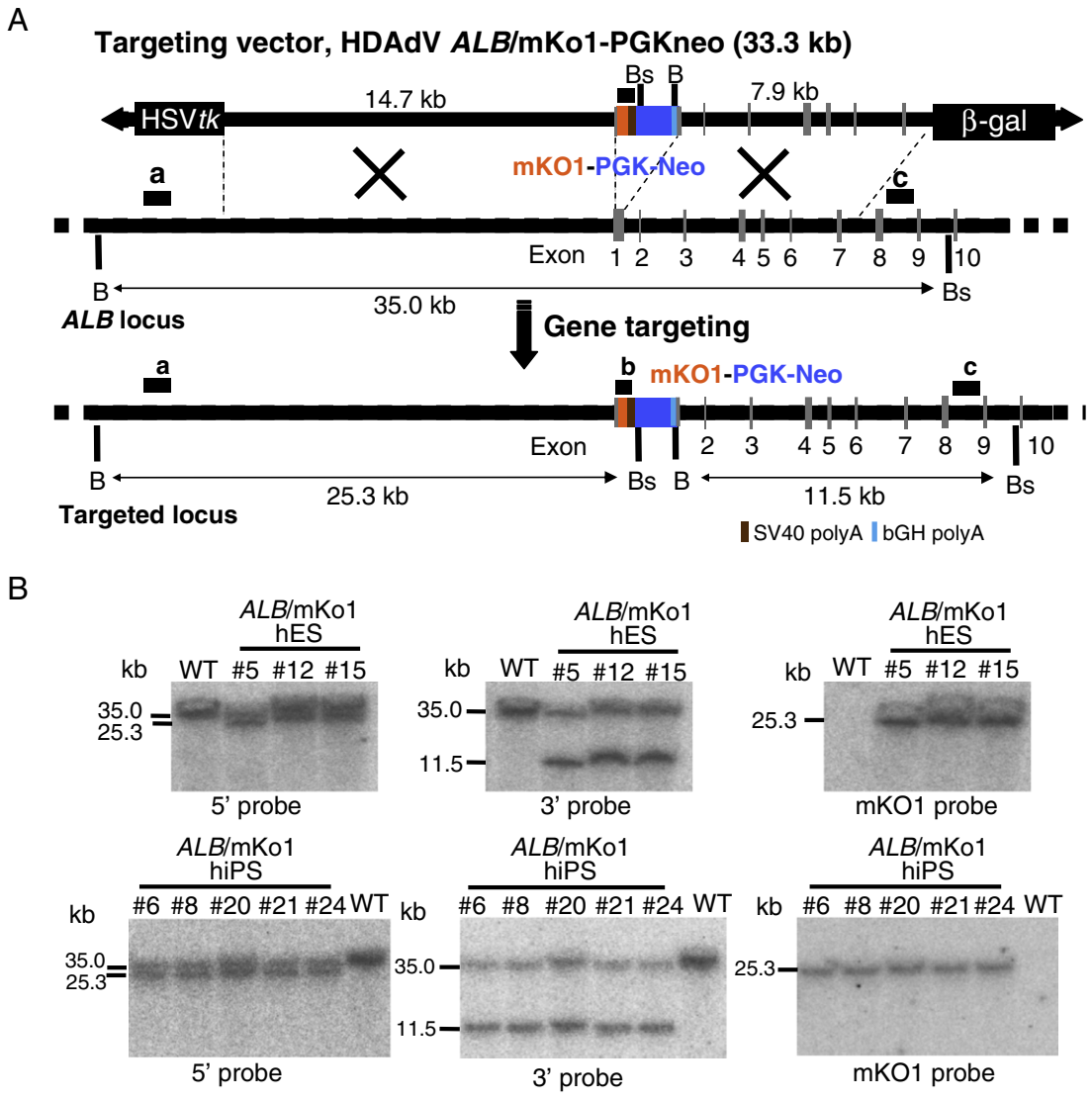

C

Strain	Infected cells	Drug selection: # of G418^R	Drug selection: # of G418^R GANC^R	Southern blot: # of analyzed	Southern blot: # of confirmed	GT per cell	GT/G418^R (%)	GT/G418^R GANC^R (%)
hESC (KhES-3)	$5.0x10^6$	16	10	9	9	$2.4x10^{-6}$	56	90
hiPSC (246H1)	$2.3x10^6$	17	6	5	5	$7.0x10^{-6}$	29	83

GT : gene targeting, GANC : ganciclovir

Figure 1 Gene targeting at the *ALB* locus in human ES/iPS cells. The strategy of gene targeting and analysis of targeted clones are shown. (A) Structure of the human *ALB* locus, the HDAdV *ALB*/mKo1-PGK-Neo targeting vector, and the targeted locus. *ALB* exons (gray boxes indicate exons 1–10) and the homology in the targeting vector are indicated by a thick line. Elements in the targeting vector include mKO1 cDNA, PGK-Neo cassette, HSV*tk*, and β-gal genes. *Bam*HI (B) and *Bsr*BI (Bs) sites are indicated. Probes a, b, and c indicate the 5′ probe, the mKO1 cDNA probe, and the 3′ probe used for Southern blot analysis, respectively. (B) Southern blot analysis of *Bam*HI- and *Bsr*BI-digested genomic DNA. *ALB*/mKo1 #5, #12, and #15 hES cells are shown in the upper panels. *ALB*/mKo1 [10, 24], #20, #21, and #24 hiPS cells are shown in the lower panels. Results with the 5′ probe, 3′ probe, and mKO1 probe are shown. (C) Gene targeting efficiencies at *ALB* locus in hES cells and iPS cells are indicated. GT, gene targeting; GANC, ganciclovir.

homologous recombination in *E. coli* (Supplementary Fig. 1). The resultant vector was named as pBC-HDAdV*ALB*/mKo1-PGKneo. A detailed subcloning description can be provided on request.

Production and purification of HDAdVs

pBC-HDAdV *ALB*/mKo1-PGKneo was linearized by PI-*Sce*I (New England Biolabs) and transfected into 293FLPe cells in

the presence of helper virus, FL helper (kindly provided by Dr. Lowenstein; Umana P). The rescued vectors were propagated by serial passages on 293FLPe cells with the addition of FL helper, as described previously (Umana et al., 2001). HDAdV DNA derived from pHDAdV *ALB*/mKo1-PGKneo was packaged into virus particles with the Ad5 fiber.

Measurement of ALB knock-in efficiencies

For infection with *ALB*-targeting HDAdVs, ES and iPS cells were plated onto 90-mm dishes coated with Matrigel on day 1 and cultured with mouse embryonic fibroblast (MEF)-conditioned

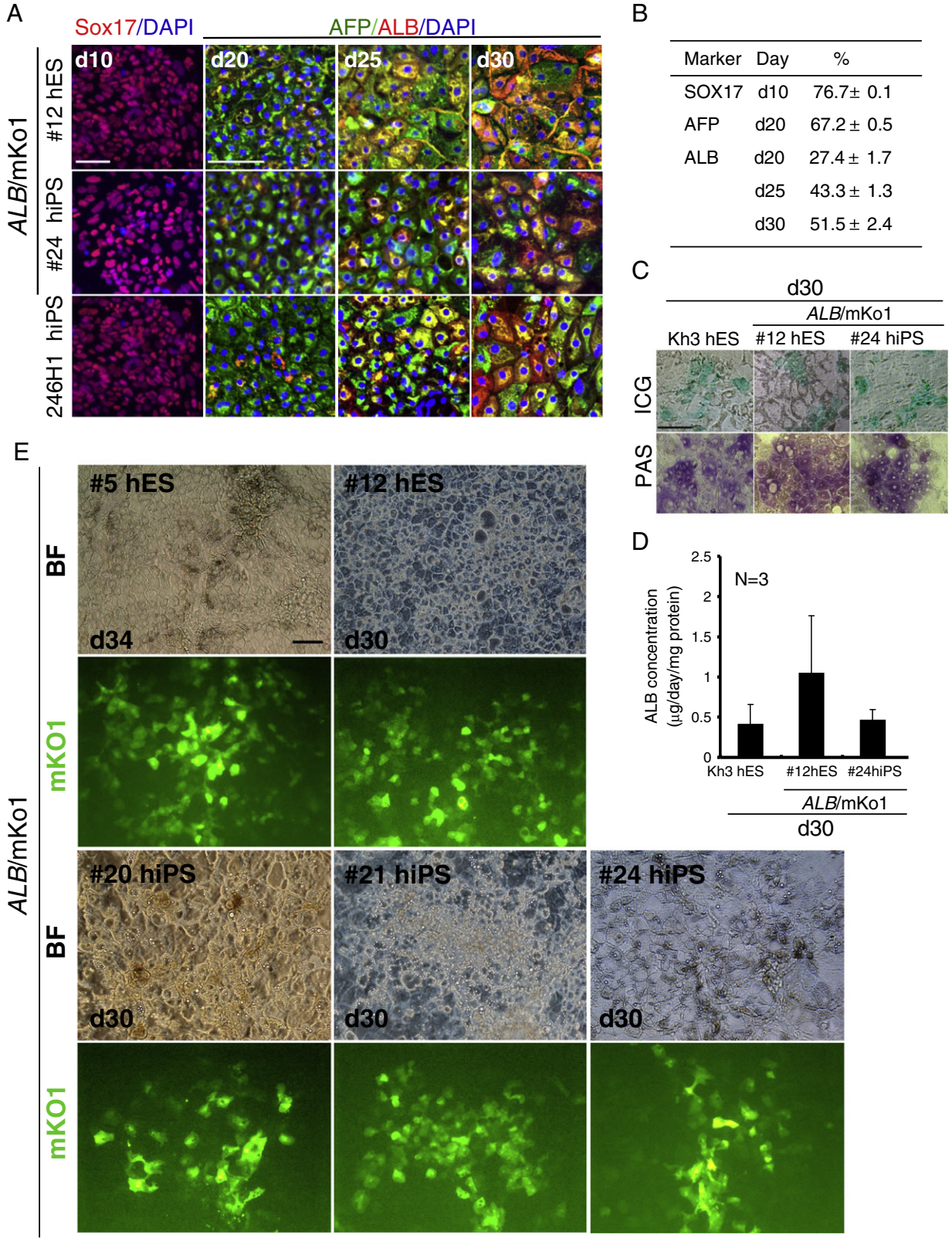

Marker	Day	%
SOX17	d10	76.7± 0.1
AFP	d20	67.2 ± 0.5
ALB	d20	27.4 ± 1.7
	d25	43.3 ± 1.3
	d30	51.5 ± 2.4

medium. On day 2, the culture medium was replaced by 1 ml of Dulbecco's modified Eagle's medium (DMEM)/F12 (Sigma-Aldrich) and the cells were counted and infected with the *ALB* targeting vectors at a multiplicity of infection of 1000 vector genomes/cell, which was determined by quantitative Southern analysis. Infection was performed for 1 h at room temperature and 8 ml of MEF-conditioned medium was added. G418 selection (50 μg/ml; Nacalai Tesque) was started 2 days after infection. After 3 weeks, surviving colonies were transferred to 96-well plates and GANC selection (2 μM, Invitrogen) was started. After 7 days, G418 and GANC double-resistant clones were characterized by Southern blot analysis.

Human ESand iPS cell lines

The hESC line KhES-3 (Suemori et al., 2006) (a gift from Dr. Nakatsuji, Kyoto University, Kyoto, Japan) and the hiPSC line 246H1 (Aizawa et al., 2012) (a gift from Dr. Yamanaka in Kyoto University, Kyoto, Japan) were used for the establishment of *ALB*/mKo1 knock-in cell lines. Human ES cells were used in accordance with the human ES cell guidelines of the Japanese government. This human ES cell work was approved by the Kumamoto University Institutional Review Board.

Undifferentiated hES and hiPS cells were maintained on a feeder layer of MEF in Knockout DMEM/F12 (Sigma-Aldrich) supplemented with 20% Knockout Serum Replacement (KSR; Invitrogen), 2 mM L-glutamine (L-Gln; Nacalai Tesque), 0.1 mM nonessential amino acids (NEAA; Invitrogen), 0.1 mM β-mercaptoethanol (ME), 50 U/ml penicillin and 50 mg/ml streptomycin (PS; Nacalai Tesque), 5 ng/ml bFGF (Peprotech) under 3% CO_2. To passage hES/iPS cells, cells were detached from the feeder layer with 0.25% trypsin and 0.1 mg/ml collagenase IV in PBS containing 20% KSR and 1 mM $CaCl_2$ at 37 °C for 6 min followed by the addition of culture medium and the disaggregation of ES/iPS clumps into smaller pieces (5–20 cells) by a cell scraper.

Immunocytochemistry

To examine the undifferentiated state of *ALB*-targeted hES and hiPS cells, the expression of Alkaline phosphatase (ALP) and surface markers (SSEA-4, TRA1-60, and TRA1-81) was examined by immunocytochemical staining with the ES cell characterization kit (Chemicon) following the manufacturer's protocol. The expression of Oct-3/4 was examined by immunocytochemical staining using the anti-OCT4 antibody (Santa Cruz Biotechnology). For immunocytochemical analyses of Sox17, ALB, and AFP, goat anti human Sox17 (R&D Systems), goat anti-human ALB (Sigma-Aldrich) and rabbit anti-human AFP (Dako Cytomation) were used. Alexa 568-conjugated, Alexa 488-conjugated, or Alexa 633-conjugated (Molecular Probes) secondary antibodies were used. To allow co-detection with mKO1, the expression levels of AFP and ALB were visualized by the Alexa 633-conjugated antibody for AFP or the Alexa 488-conjugated antibody for ALB. Cells were counterstained with 6-diamidino-2-phenylindole (DAPI) (Roche Diagnostics).

Teratoma formation

ALB-targeted hES and hiPS cells were injected subcutaneously (s.c.) into SCID mice (CLEA Japan) at an approximate total of 1×10^7 cells per clone. After 2–3 months, the resulting teratomas were recovered, fixed, and stained with hematoxylin and eosin.

Hepatic differentiation of human ES and iPS cells

For differentiation studies, hES and hiPS cells were seeded in 24-well plates pre-plated with M15 cells and cultured in differentiation medium. For days 0–10 of differentiation, RPMI 1640 medium (Invitrogen) supplemented with L-Gln, PS, NEAA, β-ME, 2% (v/v) B27 supplement (Invitrogen) and Activin A (100 ng/ml) was used. For differentiation from d10 to the indicated day, DMEM supplemented with L-Gln, PS, NEAA, β-ME, 10% KSR, 2000 mg/ml glucose, 1 μM dexamethasone (Dex; Sigma-Aldrich), and 10 ng/ml recombinant human hepatocyte growth factor (HGF, Peprotech) was used. The medium was replaced every 2 days.

Quantitative imaging analysis

Differentiated cells were assayed by immunostaining. Fluorescent images of Sox17, AFP and ALB expression and mKO1 fluorescence were quantified using a ImageXpress Micro scanning system and MetaXpress cellular image analysis software (Molecular Devices). Positive cells were counted and percentages were calculated versus total cell number, by counting DAPI stainings.

Semi-quantitative reverse-transcription polymerase chain reaction (RT-PCR) and real-time PCR analysis

RNA was extracted using the RNeasy Mini-Kit and the RNeasy Micro-Kit (Qiagen) followed by treatment with DNase I (Sigma-Aldrich). Human adult liver total RNA were purchased from Clontech Laboratories, Inc. RNA (3 μg) was reverse-

Figure 2 Differentiation of human *ALB*/mKo1 hES and iPS cells into hepatic lineages. Knock-in hES and iPS cells were confirmed to be able to differentiate into hepatic lineages showing several aspects of hepatocyte functions and expressed mKO1. (A) *ALB*/mKo1 #12 hES cells, #24 hiPS cells, and 246H1 hiPS cells were differentiated into the definitive endoderm followed by hepatic lineages. 246H1 wild type hiPS cells were used as control. A definitive endoderm marker, Sox 17, was expressed at d10. The expression of AFP and ALB was first observed at d20 and increased thereafter. AFP and ALB expression was visualized by the Alexa 633-conjugated antibody and the Alexa 488-conjugated antibody, respectively. The scale bars represent 100 μm in all panels. (B) Differentiation efficiency of *ALB*/mKo1 #12 hES cells. Proportion of cells expressing the indicated marker counted and calculated by image scanning system (N = 3) at the indicated days. (C) ICG-positive cells and PAS staining of Kh3ES and *ALB*/mKo1#12 hES cells and #24 hiPS cells on d30. KhES3 (wild type) hES cells were used as control. (D) ALB secretion by Kh3 ES and *ALB*/mKo1 #12hES cells and #24 iPS cells on d30. Error bars indicate the standard error of the mean (SEM). N = 3. KhES3 cells were used as control. (E) Fluorescence images of differentiated *ALB*/mKo1 #5 and #12 hES cells and #20, #21, and #24 hiPS cells at the indicated days are shown. Scale bars, 100 μm.

transcribed using ReverTraAce (Toyobo) and oligo dT primers (Toyobo). PCR analysis was performed as described (Shiraki et al., 2008b, 2011). For semiquantitative PCR, KOD dash polymerase (Toyobo) was used for detection of *glyceraldehyde 3-phosphate dehydrogenase* (*GAPDH*) and Amplitaq Gold fast premix (Applied Biosystems) was used for detection of the other genes. cDNA amounts and cycle numbers were optimized for detection in a linear range. The primer sequences and numbers of cycles are listed in Supplementary Table 5. The PCR conditions for each cycle were as follows: denaturation at 96 °C for 30 s, annealing at 60 °C for 2 s, extension at 72 °C for 45 s (Kod Dash polymerase) or denaturation at 96 °C for 3 s, annealing at 68 °C for 15 s, and extension at 72 °C for 45 s (Amplitaq Gold fast premix).

For real-time PCR analysis, the mRNA expression was quantified with SyberGreen on an ABI 7500 thermal cycler (Applied Biosystems, Foster City, CA). The level of each gene expression was normalized with that of *GAPDH*. The PCR conditions were as follows: denaturation at 95 °C for 15 s, annealing and extention at 60 °C for 60 s, for up to 40 cycles. Target mRNA levels were expressed as arbitrary units, and were determined using the standard curve method.

ALB secretion assay

The culture medium was replaced with fresh medium 1 day before the assay. Conditioned medium was harvested 24 h later and assayed for ALB secretion using an enzyme-linked immunosorbent assay (ELISA) kit (Bethyl, Montgomery, TX). Albumin secretion levels were normalized to the total protein of differentiated ES cells at each sampling point. The protein amounts were calculated using the Bio Rad Protein Assay Kit (Bio Rad, Hercules CA). Briefly, frozen hepatocytes obtained from Invitrogen were thawed and cultured for 24 h on collagen I-coated plates with hepatocyte maintenance medium (Invitrogen) and were subjected to the ALB secretion assay.

Indocyanine green (ICG) test

ICG (Daiichi-Sankyo Pharma, Tokyo, Japan) was diluted in the above culture medium to a final concentration of 1 mg/ml. The ICG test solution was added to the differentiated ES/iPS cells on D30, and incubated at 37 °C for 30 min. Cells were washed three times with PBS, and the cellular uptake of ICG was then examined by microscopy.

Periodic acid Schiff (PAS) analysis

The cultured cells were fixed in 3.3% formalin for 10 mins, and intracellular glycogen was stained using a PAS staining solution (Muto Pure Chemicals, Tokyo, JAPAN), according to the manufacturer's instructions.

Microscopic observation of mKO1 fluorescence

mKO1 fluorescence was detected with an excitation 546/11 nm band pass filter and the emission signal was obtained using a 555-nm-long pass dichroic mirror and a 575/30 nm band pass filter.

Flow cytometry analysis

Hoechst blue was used to verify living cells. Hoechst blue was detected with an excitation of 355 nm and detection with a 450/50 nm band pass filter. mKO1 fluorescence was analyzed with an excitation of 488 nm and detection with a 575/25 nm band pass filter. Cells were analyzed with a FACS Canto (Beckton, Dickinson and Company; BD) or purified with FACS Aria II (BD). Data were recorded with the BD FACSDiva Software program (BD) and analyzed using the FlowJo program (Tree Star).

Microarray analysis

Biotinylated cRNAs were prepared using the Gene CHIP 3′ IVT Express Kit (Affymetrix) from 50 ng of total RNA purified from ES cells on differentiation day 25 (d25) *ALB*/mKo1 negative [−], low positive [Lo], and high positive [Hi] fractions were hybridized with Human Genome U133 Plus 2.0 GeneChip arrays (Affymetrix).

All probe sets were normalized by using the MAS5.0 statistical algorithm on the Affymetrix Expression Console. Microarray results including raw signal intensities and detection calls, and adult liver data from GSM561873 of the Gene Expression Omnibus were imported into the Subio platform (Subio Inc., Japan). The intensities of the full probe sets were $\log_2$ transformed and subsequently we extracted the probe sets that were present in mKo1 [Hi] populations and whose signal intensity was more than 100 in mKO1 [Hi] populations.

Up-regulated probe sets were selected in *ALB*/mKo1 [Hi] if their [Hi]/[−] ratio showed a change more than 10-fold. Enrichment analysis by pathway was performed with all the up-regulated probe sets to identify within which specific cellular pathways these probe sets are mapped. Pathways with $p<0.05$ were considered significantly enriched. Enrichment analysis by Gene Ontology (GO) biological process terms was performed to identify specific GO terms that showed enrichment for the up-regulated probe sets. GO terms related to liver function were selected. A list of genes up-regulated in the *ALB*/mKo1 [Hi] population [Hi]/[−] ≥ 10 was entered into a Mouse Genome Informatics (MGI) batch query, and associated alleles and phenotypes of mutant mice were retrieved; the genes associated with the mutant mice that showed the liver/hepatocyte-related phenotype were extracted.

To identify drug metabolism-related genes, probe sets after filtering by detection calls and raw signal intensity, were applied to the digestive system bile secretion Kyoto Encyclopedia of Genes and Genomes (KEGG) pathway. Those probes that showed more than two-fold increase in *ALB*/mKo1 [Hi] compared to the *ALB*/mKo1 [−] population were extracted, and a heat map was generated.

To identify genes that are liver specific and/or related to liver development or maturation, the remaining genes that were not described in the above analyses were entered into the HG-U133 Plus 2.0 Sample Dataset from liver and various tissues (http://www.affymetrix.com/support/technical/sample_data/exon_array_data.affx) and GSE15238 of the Gene Expression Omnibus, consisting data sets from various stages of human liver samples (9–12 weeks fetal liver, 1-, 42- and 81-year old postnatal liver and 10 weeks whole embryo

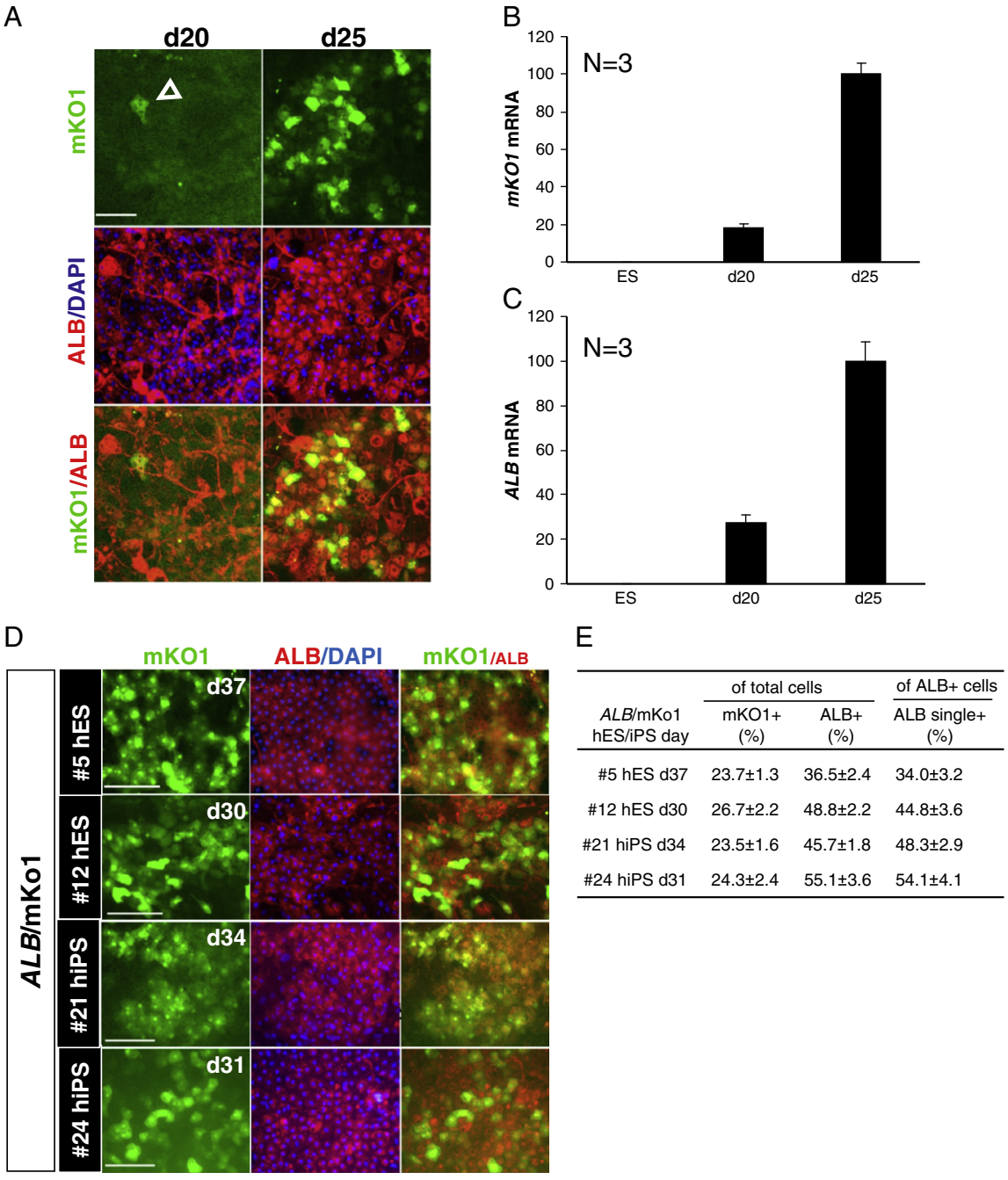

E

ALB/mKo1 hES/iPS day	of total cells mKO1+ (%)	of total cells ALB+ (%)	of ALB+ cells ALB single+ (%)
#5 hES d37	23.7±1.3	36.5±2.4	34.0±3.2
#12 hES d30	26.7±2.2	48.8±2.2	44.8±3.6
#21 hiPS d34	23.5±1.6	45.7±1.8	48.3±2.9
#24 hiPS d31	24.3±2.4	55.1±3.6	54.1±4.1

Figure 3 The onset of mKO1 expression coincides with ALB expression in *ALB*/mKo1-targeted hES and hiPS cells upon hepatic differentiation. (A) mKO1 (green) and ALB (red) expression are fist observed in *ALB*/mKo1 #12 hES cells on differentiation d20 and increased on d25, detected by immunocytochemistry. Open triangle depicts mKO1 positive cell. Scale bar, 100 μm. (B, C) Time-dependent expression of *mKO1* (B) coincides with that of *ALB* (C) on d20 and d25, detected by RT-PCR. Scale bars, 100 μm. Blue: DAPI counter-staining. (D) Merged images of mKO1 (green), anti-ALB (red), and DAPI (blue) in *ALB*/mKo1 #5 hES on d37, #12 hES cells on d30, #21 hiPS cells on d34 and #24 on d31. (E) Proportions of ALB-positive or mKO1-positive cells in total differentiated cells. ALB single positive cells within ALB-positive cells in *ALB*/mKo1 #5 hES, #12 hES, #21 hiPS and #24 hiPS cells were calculated by image scanning. Scale bars, 150 μm.

excluding the liver). Genes differentially expressed among embryonic liver samples and postnatal liver samples with more than 5-fold changes (with significance $p<0.05$) were selected.

Metabolic zonation related genes (Benhamouche et al., 2006; Torre et al., 2011) were identified from probe sets that were present in *ALB*/mKo1 [Hi] populations and whose signal intensity was more than 100 *ALB*-in mKo1 [Hi] populations and showed more than two-fold increase or decrease in *ALB*/mKo1 [Hi] compared to the *ALB*/mKo1 [−] population and a heat map was generated.

Data from human ES cells H9 and HNF4A knock-down H9 cells (GSE14897 and GSE25417 from GEO) (Si-Tayeb et al., 2010; DeLaForest et al., 2011), or AFP:eGFP-positive cells (Human Exon 1.0 ST Array)(Chiao et al, 2008) were used for

comparison. The list of gene symbols of 609 genes (Chiao et al., 2008) was entered into our microarray data and 584 genes were retrieved and 507 genes were present in *ALB*/mKo1 Hi population.

Results

Gene targeting at the *ALB* locus in human ES/iPS cells

To perform knock-in of the reporter mKO1 cDNA under the *ALB* gene promoter, we constructed an *ALB*/mKo1-targeting HDAdV vector using a BAC clone that contains the human *ALB* gene with an mKO1-PGK-Neo fragment targeted into the ATG of *ALB* exon1 (Supplementary Fig. 1). All processes were performed by homologous recombination in *Escherichia coli* (*E. coli*) using BAC vectors. The structure of the clone was verified by PCR and partial sequencing. Schematic drawings of the construction of the BAC-*ALB*/mKo1-loxP-Neo and pBC-HDAdV *ALB*/mKo1-PGK-Neo constructs are shown in Supplementary Fig. 1. To increase the gene-targeting ratio, the construct contained the herpes simplex virus thymidine kinase (HSV*tk*) gene, which allows negative selection with ganciclovir (GANC)(Fig. 1A). Human KhES-3 cells (Suemori et al., 2006) or 246H1 iPS cells (Aizawa et al., 2012) were

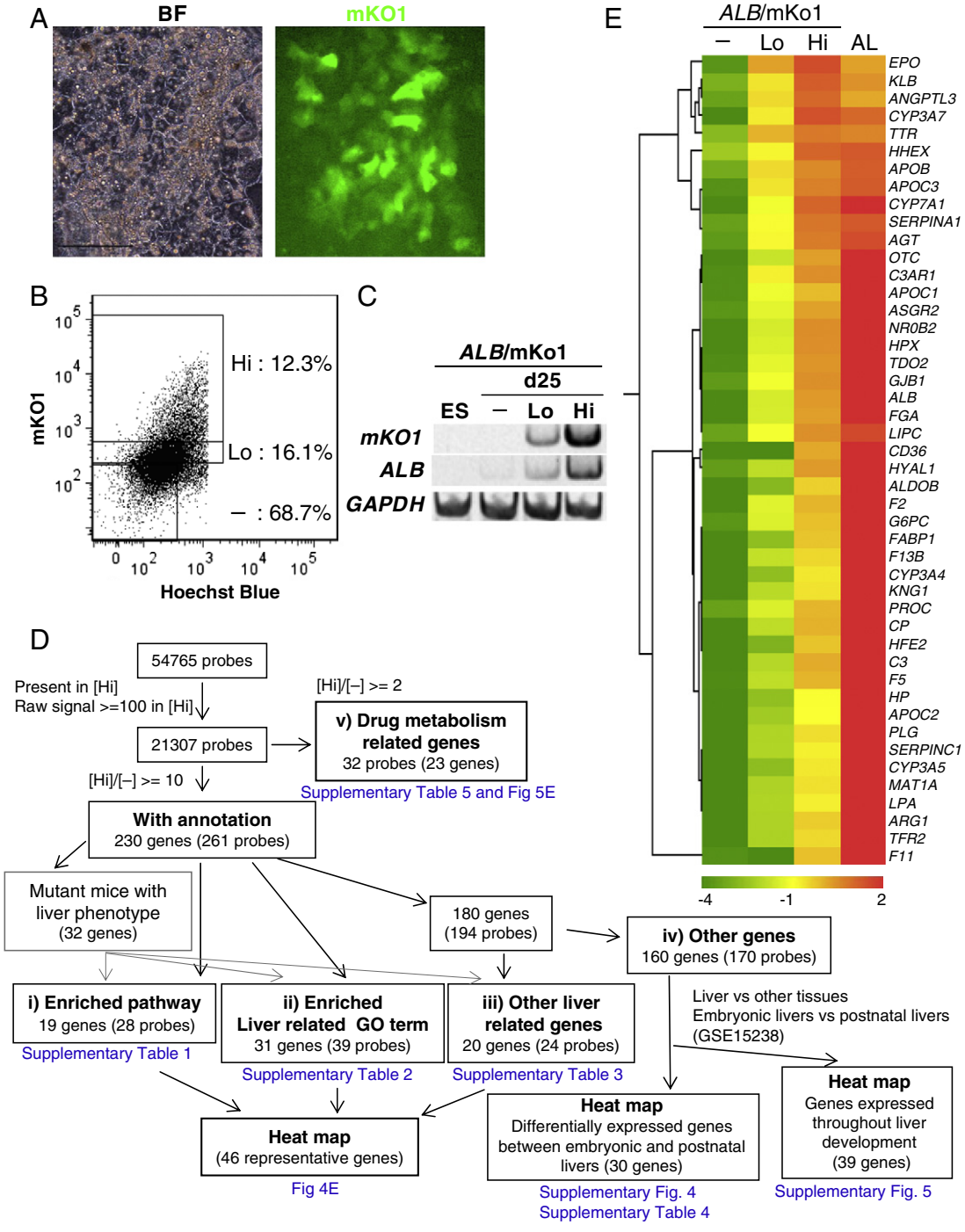

infected with the HDAdV *ALB*/mKo1-PGKneo vector, which was packaged in viral particles.

After sequential positive selection with G418 and negative selection with GANC, drug-resistant clones were analyzed and gene-targeted clones were determined. The genomic structure of the human *ALB* gene is shown in Fig. 1A. Southern blot analysis was performed to confirm that the *ALB* locus was targeted (Fig. 1B). Southern blot showed that the wild-type *ALB* allele displayed a 35.0-kb band on Southern blotting of *Bam*HI-*Bsr*BI digested DNA using the 5′ or 3′ probe (Fig. 1A, probes a and c, respectively). The *ALB*/mKo1 locus showed a 25.3-kb band with the 5′ probe and a 11.5-kb band with the 3′ probe (Fig. 1B). Furthermore, a 25.3-kb band (Fig. 1A, probe b) was detected with the mKO1 probe in the knock-in cell lines (Fig. 1B). Although the slightly fast migration profile of the #5hES clone might have been due to a difference in DNA amount and/or the long running distance and the high magnification of the gel, the possibility that deletion of small fragments occurred cannot be excluded. Of the G418-resistant 16 hES and 17 hiPS clones examined, 10 and 6 clones were GANC-resistant, of which, 9 and 5 independent clones were confirmed by southern blot analysis to have undergone a single homologous recombination event, respectively. Therefore, gene-targeting frequencies per drug-resistant colony (GANC and G418) were 90% for hES cells and 83% for hiPS cells (Fig. 1C).

The undifferentiated state and pluripotencies of the *ALB*/mKo1 knock-in cells were confirmed by their alkaline phosphatase (ALP) activities and expressions of stem cell markers such as Oct3/4, SSEA-4, TRA1-60, and TRA1-81, and teratoma formations (Supplementary Fig. 2).

Monitoring *ALB*/mKo1 knock-in hES/iPS cell differentiation into hepatic lineages

We first optimized the differentiation protocol. #12 hES and #24 hiPS cells were seeded on M15 cells and hepatic differentiation was induced, respectively. Wild-type 246H1 hiPS cells were used as a control. We added Activin A and 2% B27 in RPMI 1640 medium and cultured for 10 days to induce differentiation into the definitive endoderm and then added dexamethasone and HGF, 10% KSR in DMEM to promote hepatic differentiation. We found that our present modified protocol gave a higher proportion of SOX17-expressing endoderm, and was more efficient in yielding higher levels of *ALB* transcripts compared to our previous culture condition (Shiraki et al., 2008b) (Supplementary Fig. 3).

Under the modified protocol, immunocytochemical analysis revealed that 246H1 parental cells displayed monolayer morphologies and expressed SOX17 on day 10 (d10) (Fig. 2A). On d20 of differentiation, where most cells were AFP-positive, ALB-positive cells began to appear. ALB expression increased on d25 and further accumulated on d30 (Fig. 2A). Similar time-dependent staining patterns were observed in *ALB*/mKo1 #12 hES and #24 iPS cells (Fig. 2A, upper and middle panels). In *ALB*/mKo1 #12 hES, SOX17-positive cells were 76.7±0.1 on d10, AFP-positive cells were 67.2±0.5% on d20 and ALB-positive cells were 43.3±1.3% on d25 (Fig. 2B). These #12 hES or #24 hiPS cell-derived hepatic cells incorporated indocyanine green (ICG) and were positive for periodic acid-Schiff (PAS), which indicated cytoplasmic glycogen storage (Fig. 2C). Moreover, the secreted ALB proteins were between the range of 408–1048 ng $day^{-1}\cdot mg\cdot protein^{-1}$ detected on d30, approximately half of that of the primary hepatocytes (1865 ng $day^{-1}\cdot mg\cdot protein^{-1}$; NS, unpublished) (Fig. 2D).

The above results demonstrated that the targeted hES/iPS cells were successfully differentiated into hepatic cells displaying hepatic functions. We then examined the mKO1 fluorescence of these mKO1 targeted hES/iPS clones. *ALB*/mKo1 #5 and #12 hES cells and #20, #21 and #24 hiPS cells showed a substantial level of mKO1 fluorescence after directed for hepatic differentiation on d30–d34 (Fig. 2E).

The time-dependent mKO1 fluorescence of *ALB*/mKo1 #12 hES appeared from d20, and increased thereafter, and 18.3±1.96% of total cells became mKO1-positive on d25 (Fig. 3A, upper panels). ALB protein was detectable on d20 and continued to increase, with many positive cells on d25 (Fig. 3A). The *mKO1* transcript findings revealed by quantitative RT-PCR were consistent with the mKO1 fluorescence, which was low on d20 and increased on d25 (Fig. 3B). *ALB* mRNA also increased from d20 to d25 (Fig. 3C). mKO1 expression merged with ALB expression. We then compared with other hES/iPS clones (Fig. 3D). We counted the

Figure 4 Isolation and characterization of *ALB*/mKo1-positive cells. Differentiated cells expressing mKO1 are isolated by flow cytometry. We confirmed that cells expressed a high level of mKO1 (*ALB*/mKo1 [Hi]) also highly expressed *ALB* mRNA, and genes that characterize the adult hepatocytes. (A) Bright field (BF) and fluorescent images (mKO1) of *ALB*/mKo1 #12 hES cells differentiated for 25 days. Scale bars, 100 μm. (B) The differentiated #12 hES cells were analyzed by flow cytometry for mKO1 (Y-axis) and Hoechst blue (X-axis). Numbers in parentheses indicate the proportions of mKO1-positive cells within the total ES cell culture. mKO1 negative [−], low positive [Lo], and highly positive [Hi] populations were collected. (C) Semiquantitative RT-PCR analysis was performed in undifferentiated ES cells (ES), mKO1 [−], [Lo], [Hi], to detect *mKO1* and *ALB* transcripts. *GAPDH* served as a positive control. (D) Scheme of the gene expression profiling analysis procedure. After filtering, the probe sets with more than- 10-fold increase in the *ALB*/mKo1 [Hi] population as compared to the [−] population were selected, and applied to survey for genes associated with mutant mice with the liver phenotype and enrichment analysis. Drug metabolism related genes involved in the digestive system bile secretion pathway of KEGGs were extracted from the probe sets with [Hi]/[−]≥2. The numbers of selected probes or genes in each step are indicated. (E) The heat map generated by the Subio platform of the 46 representative genes obtained from i) enrichment analysis, ii) GO term analysis, iii) phenotype search, and iv) known hepatocyte markers. The samples shown in the columns represent *ALB*/mKo1 [−], [Lo], and [Hi], and human Adult liver (AL) from GSM561873 of the Gene Expression Omnibus. Red indicates high expression and green indicates low expression. The numbers under the color bar indicate $\log_2$ transformed signal intensity.

percentages of the ALB- or mKO1-positive cells using an image scanning system and found that approximately 23.5–26.7% of total cells were positive for mKO1 fluorescence, whereas approximately 36.5–55.1% were positive for ALB (Fig. 3E). In all clones, we found that all the mKO1-expressing cells were also ALB-positive, and that no mKO1-single positive cells were observed, although 34.0–54.1% of ALB-positive cells (approximately 12.8–30.9% of total cells) were ALB-single positive (Fig. 3E).

Isolation and characterization of *ALB*/mKo1-positive cells

To confirm that the mKO1-positive cells represented ALB-positive cells, *ALB*/mKo1 #12 hES cells were harvested on d25 of differentiation (Fig. 4A) and analyzed by flow cytometry. *ALB*/mKo1-positive cells were fractionated by signal intensities of mKo1 fluorescence into the following 3 populations: *ALB*/mKo1-negative ([−], 68.7%), mKO1 low positive ([Lo], 16.1%), and mKO1 high positive ([Hi], 12.3%) cells (Fig. 4B). The sum of mKO1-positive [Hi] and [Lo] population, being accounted to 28.4% by flow cytometry, was slightly higher than that of the mKO1-positive cells accounted by microscopic observation of the fixed cells on d25 (18.3 ± 1.96%; Fig. 3A). Semiquantitative RT-PCR analysis indicated that the *mKO1* transcript was detected as a strong band in the *ALB*/mKo1 [Hi] population but was faint in the *ALB*/mKo1 [Lo] population (Fig. 4C). Therefore, we concluded that *ALB* transcript expression correlated with mKO1 fluorescence intensity: a higher level of *ALB* transcript was expressed in mKO1 [Hi], and a lower level of *ALB* transcript was expressed in the mKO1 [Lo] population (Figs. 4B, C), and that *ALB*/mKo1 cells represent cells actively transcribing *ALB*.

Gene expression profiling analyses

We subsequently sorted *ALB*/mKo1-positive cells and performed gene expression profiling analysis of *ALB*/mKo1 [−], [Lo], and [Hi] populations (Figs. 4D, E). The following *i)–v)* analyses were performed for probe sets: *i)–iv)* with ≥10 fold increase ([Hi]/[−]≥10; 230 genes), *iv)* partially with ≥3 fold ([Hi]/[−]≥3), and *v)* with ≥2 fold increases ([Hi]/[−]≥2).

i) *Enrichment analysis by pathway*
Enrichment analysis identified 5 pathways (28 probes or 19 genes) significantly enriched in the *ALB*/mKo1 [Hi] population including the statin pathway, angiotensin-converting enzyme (ACE) inhibitors, blood clotting cascade, glycolysis and glycogenesis pathway, and irinotecan pathway (Supplementary Table 1).

ii) *Enrichment analysis by GO term and selection of liver-related genes*
From enrichment analysis by GO term, we then extracted 39 probe sets (31 genes) that are related to liver function. These consisted of genes that are related to lipid metabolism and transport, cellular iron ion homeostasis, the acute-phase reaction, complement activation, and fibrinolysis (Supplementary Table 2).

iii) *Other liver related or genes with liver phenotypes in their mutant mice*
Thirty-three genes reportedly associated with mutant mice showing hepatocyte/liver-related phenotypes were retrieved from MGI database. Among these genes, 16 genes are shown in Supplementary Tables 1 and 2. The remaining 17 genes that showed phenotypes in mutant mice, together with hepatocyte markers *Cytochrome P4503A7* (*Cyp3A7*), *tryptophan 2,3-dioxygenase* (*TDO2*), *asialoglycoprotein receptor* (*ASGR*), and *transthyretin* (*TTR*) that were not reported with liver phenotypes, are shown in Supplementary Table 3.
From the above mentioned genes, 46 representative genes were used to generate a heat map using the Subio program (Fig. 4E).

iv) *Genes differentially or constitutively expressed during liver developmental and after birth*
We then analyzed the remaining 160 genes (referred as 'other genes', Fig. 4D), and compared with data sets (GSE15238 of the Gene Expression Omnibus) from early stages of human liver development (9–12 weeks human embryonic livers) and postnatal livers (1, 42, 81 years) and with HG-U133 Plus 2.0 Sample Dataset from liver and various tissues (http://www.affymetrix.com/support/technical/sample_data/exon_array_data.affx).
Thirty genes that are differentially expressed during liver developmental stages are listed in Supplementary Fig. 4. Of these genes, 14 were absent in the embryonic livers, but increased later in the adult liver, and were enriched in *ALB*/mKo1[Hi] population with ≥3-fold increase (*ALB*/mKo1[Hi]/[−]≥3) (Supplementary Table 4). We actually confirmed that *ZG16* and *CHST9* are specifically expressed in the adult liver (K.U. unpublished). Thirty-nine genes that are expressed throughout developmental stages of liver are shown in Supplementary Fig. 5. Of these genes, genes specifically expressed in the liver are listed in red letters.

v) *Drug metabolism-related genes*
From probe sets that were up-regulated ≥two-fold in the *ALB*/mKo1 [Hi] compared to the *ALB*/mKo1 [−] population ([Hi]/[−]≥2), important genes for hepatic drug metabolism were extracted (32 probe sets or 23 genes, Supplementary Table 5). A heat map of 21 genes that are expressed in the hepatocyte was generated to compare with those of the adult liver (Fig. 5). Enzymes involved in phase I metabolism (bile acid synthesis and detoxification), phase II metabolism (conjugation) or sinusoidal transporters (efflux or uptake), and bile canalicular transporters were enriched.
We then confirmed the gene expression profiles with other clones (Fig. 6). We found that *ALB*/mKo1#5 hES cells were less potent and *ALB*/mKo1-positive cells began to appear on d25. Therefore, we considered *ALB*/mKo1#5 hES d35 to be comparable with d25 #12hES, and #24hiPS d34 be comparable with #12 hiPS d34. We fractionated *ALB*/mKo1 [Hi], [Lo] and [−] populations by flow cytometry from *ALB*/mKo1 #5 hES (d35) and #24hiPS (d34) and compared with #12 hES d25 and d34 (Figs. 6B, C). Representative genes identified in the above microarray analyses were picked up and their expressions were confirmed by semi-quantitative RT-PCR analyses. All genes examined were expressed at a much higher level in *ALB*/mKo1 [Hi] compared to [−] population. Taken together, we

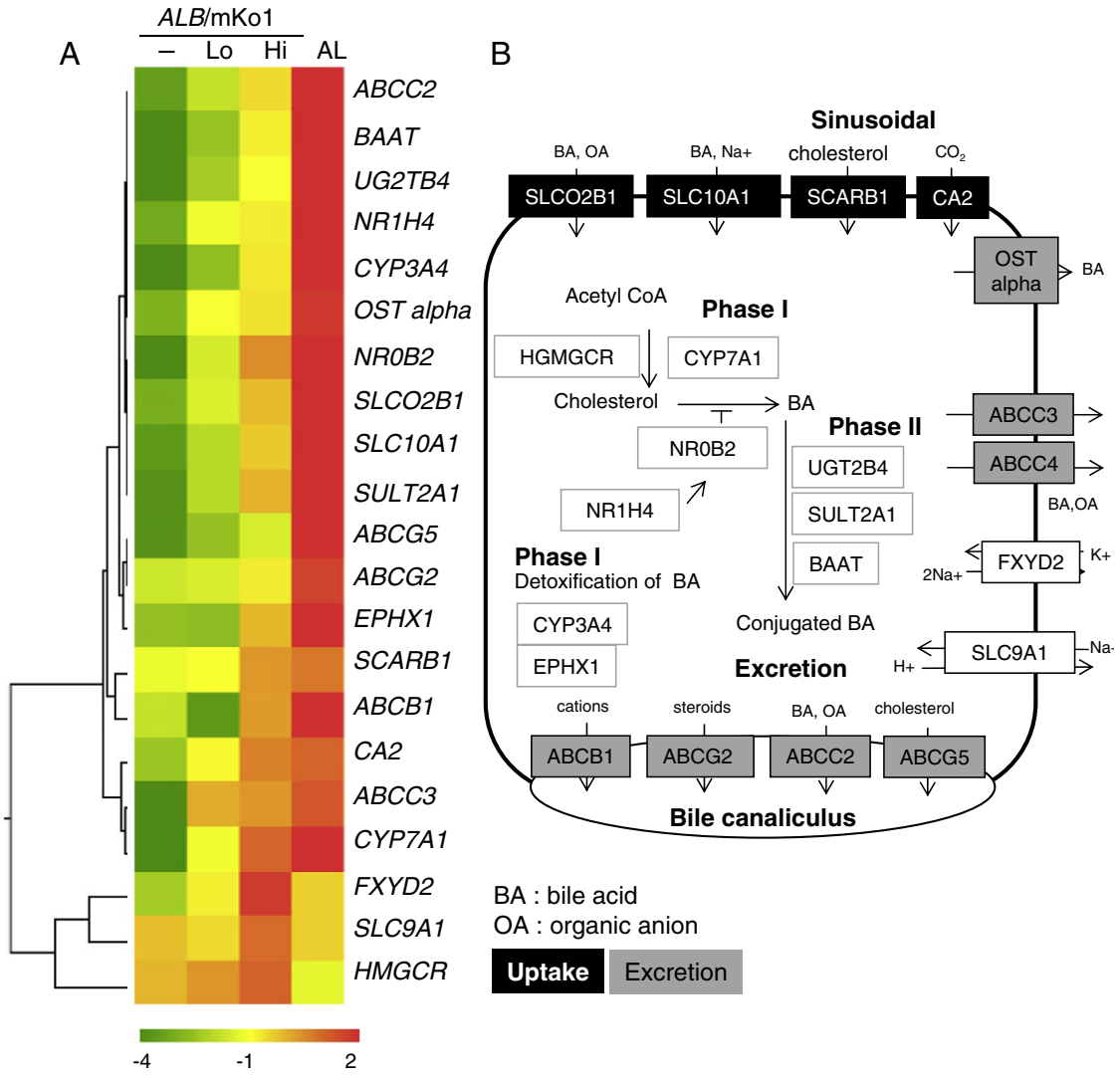

Figure 5 Drug metabolism-related genes are enriched in the *ALB*/mKo1 [Hi] population. (A) A heat map of the 21 genes generated from a search for drug metabolism-related genes expressed in the hepatocytes that were up-regulated ≥2-fold in the *ALB*/mKo1 [Hi] population as compared to the *ALB*/mKo1 [–] population. The samples shown in the columns represent *ALB*/mKo1 [–], [Lo], and [Hi] and human AL (adult liver). Red indicates high expression, and green indicates low expression. The numbers under the color bar indicate $\log_2$ signal intensity. (B) Schematic drawings of the functions of the genes shown in (A), which function as transporters and phases I and II enzymes in drug metabolism. Uptake transporters and excretion transporters are indicated by black boxes and gray boxes, respectively.

concluded that similar enrichments of the mature functional hepatocyte genes are observed in all *ALB*/mKo1 [Hi] populations of the hES/iPS clones so far examined.

Discussion

HDAdV achieved highly efficient gene targeting for *ALB*/mKo1 in human ES and iPS cells

Homologous recombination has been used widely in mouse ES cells and has contributed to biological studies, but significant efficiency differences between mice and humans have hampered its application to hES cells (Thomas and Capecchi, 1987). Presently, several reports have described alternative gene modification in hES by homologous recombination and the reported efficiency by conventional electroporation method is low in both hES and hiPS cells (0.14–0.24%) (Zwaka and Thomson, 2003; Zou et al., 2009). We previously reported that the HDAdV system is a powerful tool for genetic manipulation of hES/iPS cells other than mouse ES cells (Suzuki et al., 2008; Aizawa et al., 2012). In our previous report with the HDAdV system, chromosomal integration efficiency of the hypoxanthine phosphoribosyl transferase1 (HPRT1) was ~5.6×10^{-5}/cell and gene targeting/chromosomal integration was 3–55% in hES cells whereas chromosomal integration efficiency by use of the same vector was 1.6×10^{-6}/cell and gene targeting/chromosomal random integration was ~0.58% in the case of electroporation. In this report, the targeting/chromosomal integration ratio was as high as 56% for hES and 29% for hiPS cells. When combined with negative selection, the frequencies were enriched up to 90% for hES cells and 83% for hiPS cells

(Fig. 1C). Our results thus demonstrate that HDAdVs is a powerful technology for gene targeting in human ES/iPS cells.

Recently, the lentivirus vector system was utilized to isolate hepatic cells from human ES cells [Duan et al., 2007; Chiao et al., 2008]. The differentiated human ES cells were enriched by

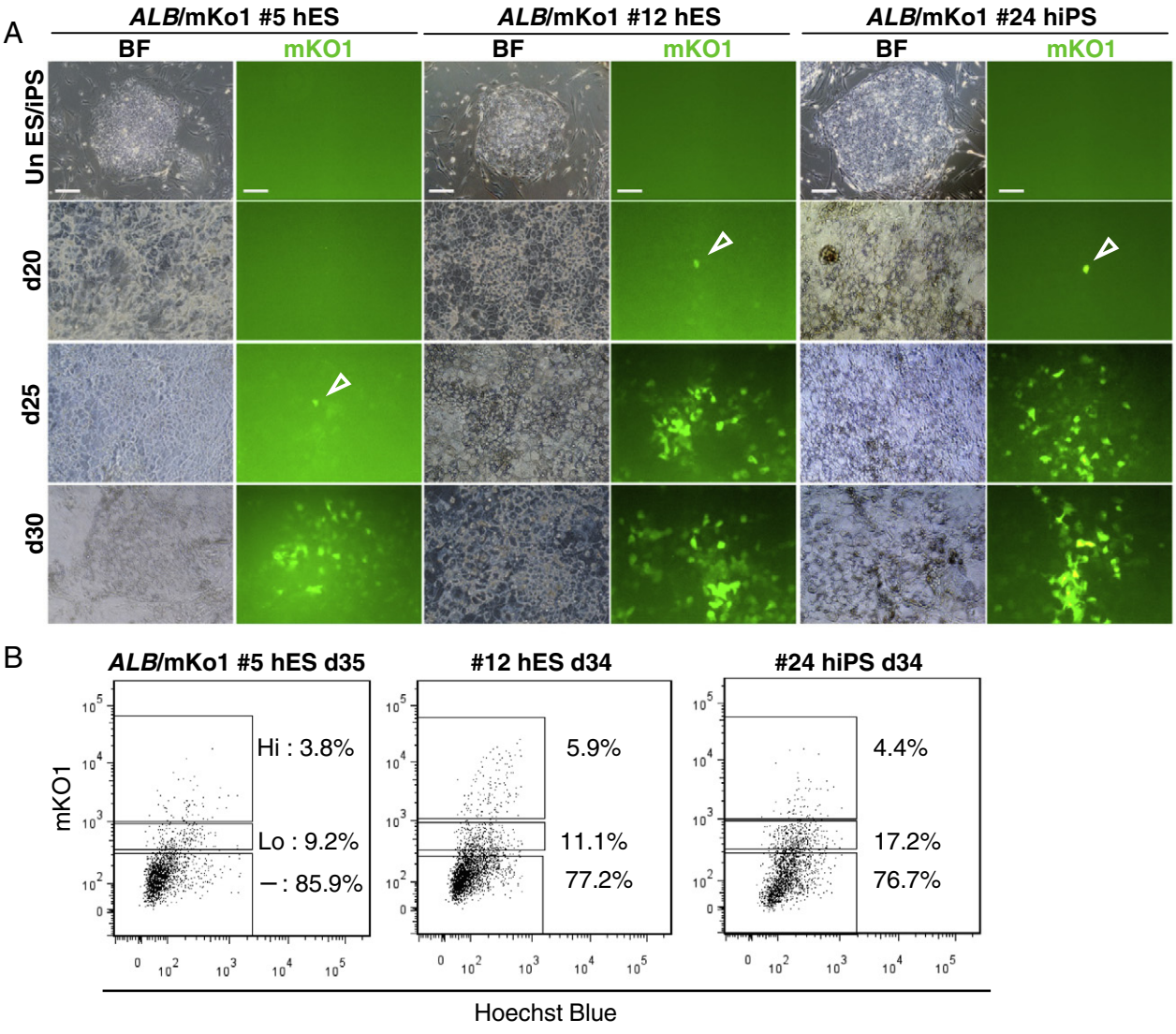

a transducing lentivirus vector containing a green fluorescent protein (GFP) reporter driven under the *α1-antitrypsin* (*AAT or SERPIN A1*) promoter (Duan et al., 2007) or enhanced GFP driven by the *AFP* promoter (Chiao et al., 2008). Since random integration occurs in the lentivirus vector system, the fidelity of the expression pattern of the transgene required to be confirmed if they recapitulate endogenous gene expression pattern. In contrast, our HDAdV system provides a highly efficient method for targeting the gene of interest by homologous recombination, in which the reporter genes consistently follow the endogenous promoter activity. Furthermore, compared to the *ALB* gene, which is tissue specifically expressed in the liver, the *AAT* gene is also expressed in the lung (Carlson et al., 1988).

Hepatic differentiation of the hES/iPS cells

We induced hepatic differentiation of hiPS and hES cells using a previously established M15 procedure with modifications to the culture medium. We observed higher proportions of SOX17-positive cells and much higher levels of *AFP* and *ALB* transcripts and mKO1 fluorescence, compared to our previously described culture condition (Shiraki et al., 2008b) (Supplementary Fig. 3). Under the modified protocol, the mKO1 fluorescence became detectable from around d20 and increased to a substantial level on d25 (Fig. 3A), whereas it was not until d30–d34 that the mKO1 fluorescence became detectable under the previous condition (data not shown). Under the modified culture condition, the *ALB*/mKo1 knock-in hiPS and hES cells differentiated into hepatic fates in vitro and yielded approximately 67.2% AFP-positive cells at d20 and 51.5% ALB-positive cells at d30 (Fig. 2B). These cells secreted ALB protein (Fig. 2D) at a level approximately one-fourth to one-half of that of the cultured human primary hepatocytes (at 1865 ng $day^{-1}\cdot mg\cdot protein^{-1}$; NS, unpublished) and showed ICG intake and positive for PAS (Fig. 2C).

Differentiated cells with mKO1 fluorescence were observed from d20 and increased on d25, which correlated with the increase of *mKO1* transcript. *ALB* transcripts and ALB protein were also detected from d20 (Fig. 3). Therefore, the onset of mKO1 and *ALB* expression coincided with each other in a time dependent manner. All the mKO1-positive cells co-expressed ALB protein and no mKO1-single positive cells were observed. However, there were ALB-single positive cells in all hES/iPS clones. This discrepancy between the mKO1- and ALB-expressing cells might due to the differences in protein stability between mKO1 and ALB. The half-life reported for native ALB protein is 19 days (Torre et al., 2011), which is much longer than that reported with the green fluorescence protein (GFP) as approximately 24 h (Li et al., 1998). Given that it is difficult to maintain functional hepatocytes in vitro in long term cultures. *ALB* transcriptional activities might change coordinately with the hepatocyte activities. The extended stability of the ALB protein then results in a prolonged ALB protein accumulation in cells with low *ALB* transcriptional activities.

Expression profile analysis of the hES cell-derived *ALB*/mKo1-positive cells

Isolation and analyses of the *ALB*/mKo1-positive populations revealed that *ALB*/mKo1[Hi] populations actively transcribe *ALB* compared to *ALB*/mKo1[Lo] population (Fig. 4A). Through expression profile analysis of the isolated hES cell-derived *ALB*/mKo1[Hi], [Lo], and [−] populations, we found that many genes responsible for hepatocyte-like characteristics were up-regulated in the *ALB*/mKo1[Hi] population as compared to the *ALB*/mKo1[−] population (Supplementary Tables 1–5). The liver plays a major role in metabolism (amino acid synthesis, metabolism of carbohydrates, proteins, and lipids), iron storage, production of coagulation factors, and immunological molecules or hormones and is a major tissue for drug metabolism. In addition to producing functional proteins, nuclear receptors that function as transcription factors and play regulatory roles are also up-regulated in the *ALB*/mKo1 [Hi] population as compared to the *ALB*/mKo1[−] population. Among the genes that were enriched in the hES-derived *ALB*/mKo1[Hi] population, there are many genes in which targeted mutations in mice resulted in liver phenotypes (Supplementary Tables 1–3).

Wnt/β-catenin signaling is shown to direct liver metabolic zonation (Benhamouche et al., 2006; Torre et al., 2011). *APC2* gene together with several periportal and perivenous genes were enriched, and several *Wnts* are down-regulated in the *ALB*/mKo1[Hi] population, thereby suggesting that genes that play a role in metabolic zonation are actively expressed in *ALB*/mKo1[Hi] population (Supplementary Fig. 6).

We also compared our microarray data with other's data derived from human ES cells H9 and HNF4A knock-down H9 cells (GSE14897 and GSE25417 from GEO, (Si-Tayeb et al., 2010; DeLaForest et al., 2011)). Of the 297 up-regulated probe sets in the differentiated H9 cells, 266 probe sets are not enriched in the *ALB*/mKo1[Hi] population (Supplementary Fig. 7A). GO terms enriched in these 266 probe sets are those related to lineages other than the liver, which are in similarity with our *ALB*/mKo1 [−] population (data not shown). By contrast, a high proportion of liver specific genes (22 out of 28) down-regulated in the HNF4A knock-down cells are enriched in the *ALB*/mKo1 [Hi] population (Supplementary Fig. 7A). We also compared our microarray profiling results with that of the AFP:eGFP-positive cells reported previously (Chiao et al., 2008) (Supplementary Fig. 7B). Approximately1/10 of the 507 probe sets enriched in the AFP:eGFP-positive cells, such as *ALB*, *transferrinn (TF)* and *TTR*, are overlapped with those in *ALB*/mKo1 [Hi]/[−] ≥ 10. Genes, such as *CYP3A4*, *CYP3A7*, *HHEX*, *MAT1A* and *SERPINA1*, are only enriched in *ALB*/mKo1 [Hi]/[−] ≥ 10. *Keratin7* (*KRT7*) is one of the 460 genes

Figure 6 Examination of gene expressions in other *ALB*/mKo1 clones, of the genes enriched in the *ALB*/mKo1 [Hi] population. Gene expressions in *ALB*/mKo1 [Hi], [Lo] and [−] populations from *ALB*/mKo1 #5 hES and #24 hiPS were compared with those from #12 hES cells. (A) Time dependent mKO1 fluorescence observed in *ALB*/mKo1 #5 hES, #12 hES and #24 hiPS cells. Green: mKO1 fluorescence. (B, C) The differentiated cells were analyzed by flow cytometry for mKO1 (Y-axis) and Hoechst blue (X-axis). Numbers indicate the proportions of mKO1-positive cells within the total ES cell culture. mKO1 negative [−], low positive [Lo], and highly positive [Hi] populations were collected. (D) Semi-quantitative RT-PCR analyses were performed in undifferentiated ES cells (ES), mKO1 [−], [Lo], [Hi], to detect representative enriched genes from microarray results. *GAPDH* served as a positive control. Scale bars, 100 μm.

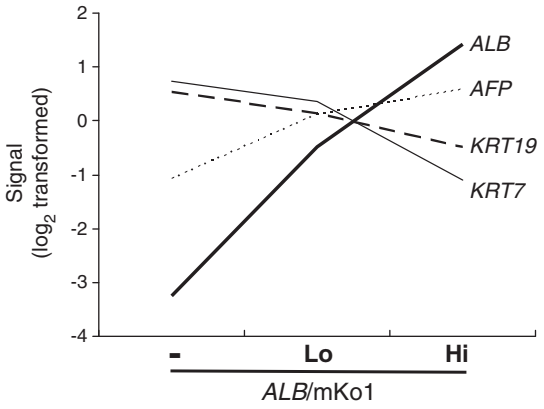

Gene Title	Symbol	[Hi]/[-]	[Lo]/[-]
keratin 19	KRT19	0.5	0.7
keratin 7	KRT7	0.3	0.8
alpha-fetoprotein	AFP	3.1	2.3
albumin	ALB	25.1	6.7

Figure 7 Cholangiocyte lineage markers *Keratin7*, *Keratin19* and hepatoblast marker *AFP* expression levels in the three hiPS cell-derived populations. *Keratin 7*, *19* are down-regulated, while *AFP*, *ALB* genes are up-regulated in the *ALB*/mKo1 [Hi] population.

specifically enriched in the AFP:eGFP-positive cells, but not in *ALB*/mKo1 [Hi]/[−] ≥ 10.

In our present study, *AFP* is enriched by 3.1- or 2.3-fold in *ALB*/mKo1 [Hi]/[−] or [Lo]/[−], respectively. *KRT7* or *KRT19*, cholangiocyte markers are down-regulated in *ALB*/mKo1 [Hi]/[−] (Fig. 7). Taken together, the present *ALB*/mKo1 [Hi] represents cells of hepatocyte lineage rather than immature hepatoblast lineage.

As described above, liver specific genes and/or differentially expressed during liver development could be examined by studying the hES and hiPS cells derived *ALB*/mKo1-positive cells. However, besides the genes that are up-regulated in postnatal livers, some of the genes that are normally down-regulated in postnatal liver are still expressed in the *ALB*/mKo1[Hi]. This result therefore suggests that the differentiated cells are not fully mature and further studies for the repression of such genes might lead to the derivation of more matured hepatocytes. Moreover, in spite of many genes associated with mature hepatocyte are enriched in the *ALB*/mKo1[Hi] populations, genes such *MRP4* (sinusoidal efflux transporters), *BSEP* (canalicular transporters), *CYP2C9*, *CYP2C19*, *OATP1B1*, and *OATP1B3*, were not enriched, and would require further improvement of the differentiation procedure for obtaining more mature hepatocytes.

OATP1B1 and OATP1B3 are considered to be liver specific transporters. Targeting of additional reporters into the locus of these genes in *ALB*/mKo1 hES/iPS would be helpful for visualization of further hepatocyte maturation and enable screening of chemicals that potentiate differentiation. In this study, we performed targeting to knock-in a mKO1 cassette into *ALB* gene loci in human ES and iPS cells. The genetically tagged cells are shown to be valuable for monitoring in vitro differentiation into hepatic cells, and allow isolation of cells that actively express *ALB* at a transcriptional but not translational level. Analysis of the *ALB*/mKo1-positive cells revealed that cells actively transcribing *ALB* correlate to their ability to express characteristic marker genes of the adult human hepatocytes. Similar enrichments of the characteristic marker genes in *ALB*/mKo1 [Hi] populations were confirmed in different knock-in clones established in this study (Fig. 6).

Our results therefore reinforced the advantage of using the present *ALB*/mKo1 knock-in hES/iPS cell lines for gaining further insights into the differentiation and characterization of hES/iPS cell-derived hepatocytes.

Acknowledgments

We thank Drs. Nakatsuji and Yamanaka (Kyoto University) for providing hES and hiPS cell lines, Dr. Pedro R. Lowenstein (Cedars-Sinai Medical Center) for providing 293FLPe cells and FL helper virus, Dr. Neal G. Copeland (National Cancer Institute) for providing the *E. coli* strains and plasmids for BAC recombineering, and Drs. Takeda and Yusa (Osaka University) for p23-loxP-Zeo plasmid. We thank Ms. Akiko Harada, Yuzuru Iwanaga, and members of the Gene Technology Center at Kumamoto University for technical assistance. This work was supported by a grant (to S.K. and K.M) from the New Energy and Industrial Technology Development Organization (NEDO) and a grant from the National Institute of Biomedical Innovation (to NS). This work was also supported in part by a funding program for Next Generation World-Leading Researchers (NEXT Program) from the Japan Society for the Promotion of Science (JSPS) (to S.K.) and a Global COE grant from the Ministry of Education, Culture, Sports, Science and Technology (MEXT). S.K. is a global COE member.

Appendix A. Supplementary data

Supplementary data to this article can be found online at http://dx.doi.org/10.1016/j.scr.2012.11.003.

References

Aizawa, E., Hirabayashi, Y., Iwanaga, Y., Suzuki, K., Sakurai, K., Shimoji, M., Aiba, K., Wada, T., Tooi, N., Kawase, E., Suemori, H., Nakatsuji, N., Mitani, K., 2012. Efficient and accurate homologous recombination in hESCs and hiPSCs using helper-dependent adenoviral vectors. Mol. Ther. 20, 424–431.

Belmonte, J.C., Ellis, J., Hochedlinger, K., Yamanaka, S., 2009. Induced pluripotent stem cells and reprogramming: seeing the science through the hype. Nat. Rev. Genet. 10, 878–883.

Benhamouche, S., Decaens, T., Godard, C., Chambrey, R., Rickman, D.S., Moinard, C., Vasseur-Cognet, M., Kuo, C.J., Kahn, A., Perret, C., Colnot, S., 2006. Apc tumor suppressor gene is the "zonation-keeper" of mouse liver. Dev. Cell 10, 759–770.

Cai, J., Zhao, Y., Liu, Y., Ye, F., Song, Z., Qin, H., Meng, S., Chen, Y., Zhou, R., Song, X., Guo, Y., Ding, M., Deng, H., 2007. Directed differentiation of human embryonic stem cells into functional hepatic cells. Hepatology 45, 1229–1239.

Carlson, J.A., Rogers, B.B., Sifers, R.N., Hawkins, H.K., Finegold, M.J., Woo, S.L., 1988. Multiple tissues express alpha 1-antitrypsin in transgenic mice and man. J. Clin. Invest. 82, 26–36.

Chiao, E., Elazar, M., Xing, Y., Xiong, A., Kmet, M., Millan, M.T., Glenn, J.S., Wong, W.H., Baker, J., 2008. Isolation and transcriptional profiling of purified hepatic cells derived from human embryonic stem cells. Stem Cells 26, 2032–2041.

Copeland, N.G., Jenkins, N.A., Court, D.L., 2001. Recombineering: a powerful new tool for mouse functional genomics. Nat. Rev. Genet. 2, 769–779.

Davila, J.C., Cezar, G.G., Thiede, M., Strom, S., Miki, T., Trosko, J., 2004. Use and application of stem cells in toxicology. Toxicol. Sci. 79, 214–223.

DeLaForest, A., Nagaoka, M., Si-Tayeb, K., Noto, F.K., Konopka, G., Battle, M.A., Duncan, S.A., 2011. HNF4A is essential for specification of hepatic progenitors from human pluripotent stem cells. Development 138, 4143–4153.

Di, Domenico A.I., Christodoulou, I., Pells, S.C., McWhir, J., Thomson, A.J., 2008. Sequential genetic modification of the hprt locus in human ESCs combining gene targeting and recombinase-mediated cassette exchange. Cloning Stem Cells 10, 217–230.

Duan, Y., Catana, A., Meng, Y., Yamamoto, N., He, S., Gupta, S., Gambhir, S.S., Zern, M.A., 2007. Differentiation and enrichment of hepatocyte-like cells from human embryonic stem cells in vitro and in vivo. Stem Cells 25, 3058–3068.

Evans, M.J., Kaufman, M.H., 1981. Establishment in culture of pluripotential cells from mouse embryos. Nature 292, 154–156.

Hay, D.C., Zhao, D., Fletcher, J., Hewitt, Z.A., McLean, D., Urruticoechea, Uriguen A., Black, J.R., Elcombe, C., Ross, J.A., Wolf, R., Cui, W., 2008a. Efficient differentiation of hepatocytes from human embryonic stem cells exhibiting markers recapitulating liver development in vivo. Stem Cells 26, 894–902.

Hay, D.C., Fletcher, J., Payne, C., Terrace, J.D., Gallagher, R.C., Snoeys, J., Black, J.R., Wojtacha, D., Samuel, K., Hannoun, Z., Pryde, A., Filippi, C., Currie, I.S., Forbes, S.J., Ross, J.A., Newsome, P.N., Iredale, J.P., 2008b. Highly efficient differentiation of hESCs to functional hepatic endoderm requires ActivinA and Wnt3a signaling. Proc. Natl. Acad. Sci. U. S. A. 105, 12301–12306.

Karasawa, S., Araki, T., Nagai, T., Mizuno, H., Miyawaki, A., 2004. Cyan-emitting and orange-emitting fluorescent proteins as a donor/acceptor pair for fluorescence resonance energy transfer. Biochem. J. 381, 307–312.

Katsumoto, K., Shiraki, N., Miki, R., Kume, S., 2010. Embryonic and adult stem cell systems in mammals: ontology and regulation. Dev. Growth Differ. 52, 115–129.

Kaufman, M.H., Robertson, E.J., Handyside, A.H., Evans, M.J., 1983. Establishment of pluripotential cell lines from haploid mouse embryos. J. Embryol. Exp. Morphol. 73, 249–261.

Li, X., Zhao, X., Fang, Y., Jiang, X., Duong, T., Fan, C., Huang, C.C., Kain, S.R., 1998. Generation of destabilized green fluorescent protein as a transcription reporter. J. Biol. Chem. 273, 34970–34975.

Li, M., Suzuki, K., Qu, J., Saini, P., Dubova, I., Yi, F., Lee, J., Sancho-Martinez, I., Liu, G.H., Izpisua, Belmonte J.C., 2011. Efficient correction of hemoglobinopathy-causing mutations by homologous recombination in integration-free patient iPSCs. Cell Res. 21, 1740–1744.

Liu, G.H., Suzuki, K., Qu, J., Sancho-Martinez, I., Yi, F., Li, M., Kumar, S., Nivet, E., Kim, J., Soligalla, R.D., Dubova, I., Goebl, A., Plongthongkum, N., Fung, H.L., Zhang, K., Loring, J.F., Laurent, L.C., Izpisua, Belmonte J.C., 2011. Targeted gene correction of laminopathy-associated LMNA mutations in patient-specific iPSCs. Cell Stem Cell 8, 688–694.

Ohbayashi, F., Balamotis, M.A., Kishimoto, A., Aizawa, E., Diaz, A., Hasty, P., Graham, F.L., Caskey, C.T., Mitani, K., 2005. Correction of chromosomal mutation and random integration in embryonic stem cells with helper-dependent adenoviral vectors. Proc. Natl. Acad. Sci. U. S. A. 102, 13628–13633.

Osoegawa, K., Mammoser, A.G., Wu, C., Frengen, E., Zeng, C., Catanese, J.J., de Jong, P.J., 2001. A bacterial artificial chromosome library for sequencing the complete human genome. Genome Res. 11, 483–496.

Palmer, D.J., Ng, P., 2005. Helper-dependent adenoviral vectors for gene therapy. Hum. Gene Ther. 16, 1–16.

Ruby, K.M., Zheng, B., 2009. Gene targeting in a HUES line of human embryonic stem cells via electroporation. Stem Cells 27, 1496–1506.

Sakurai, K., Shimoji, M., Tahimic, C.G., Aiba, K., Kawase, E., Hasegawa, K., Amagai, Y., Suemori, H., Nakatsuji, N., 2010. Efficient integration of transgenes into a defined locus in human embryonic stem cells. Nucleic Acids Res. 38, e96.

Shiraki, N., Yoshida, T., Araki, K., Umezawa, A., Higuchi, Y., Goto, H., Kume, K., Kume, S., 2008a. Guided differentiation of embryonic stem cells into Pdx1-expressing regional-specific definitive endoderm. Stem Cells 26, 874–885.

Shiraki, N., Umeda, K., Sakashita, N., Takeya, M., Kume, K., Kume, S., 2008b. Differentiation of mouse and human embryonic stem cells into hepatic lineages. Genes Cells 13, 731–746.

Shiraki, N., Higuchi, Y., Harada, S., Umeda, K., Isagawa, T., Aburatani, H., Kume, K., Kume, S., 2009. Differentiation and characterization of embryonic stem cells into three germ layers. Biochem. Biophys. Res. Commun. 381, 694–699.

Shiraki, N., Yamazoe, T., Qin, Z., Ohgomori, K., Mochitate, K., Kume, K., Kume, S., 2011. Efficient differentiation of embryonic stem cells into hepatic cells in vitro using a feeder-free basement membrane substratum. PLoS One 6, e24228.

Si, Tayeb K., Lemaigre, F.P., Duncan, S.A., 2010. Organogenesis and development of the liver. Dev. Cell 18, 175–189.

Si-Tayeb, K., Noto, F.K., Nagaoka, M., Li, J., Battle, M.A., Duris, C., North, P.E., Dalton, S., Duncan, S.A., 2010. Highly efficient generation of human hepatocyte-like cells from induced pluripotent stem cells. Hepatology 51, 297–305.

Suemori, H., Tada, T., Torii, R., Hosoi, Y., Kobayashi, K., Imahie, H., Kondo, Y., Iritani, A., Nakatsuji, N., 2001. Establishment of embryonic stem cell lines from cynomolgus monkey blastocysts produced by IVF or ICSI. Dev. Dyn. 222, 273–279.

Suemori, H., Yasuchika, K., Hasegawa, K., Fujioka, T., Tsuneyoshi, N., Nakatsuji, N., 2006. Efficient establishment of human embryonic stem cell lines and long-term maintenance with stable karyotype by enzymatic bulk passage. Biochem. Biophys. Res. Commun. 345, 926–932.

Sullivan, G.J., Hay, D.C., Park, I.H., Fletcher, J., Hannoun, Z., Payne, C.M., Dalgetty, D., Black, J.R., Ross, J.A., Samuel, K., Wang, G., Daley, G.Q., Lee, J.H., Church, G.M., Forbes, S.J., Iredale, J.P., Wilmut, I., 2010. Generation of functional human hepatic endoderm from human induced pluripotent stem cells. Hepatology 51, 329–335.

Suzuki, K., Mitsui, K., Aizawa, E., Hasegawa, K., Kawase, E., Yamagishi, T., Shimizu, Y., Suemori, H., Nakatsuji, N., Mitani, K., 2008. Highly efficient transient gene expression and gene targeting in primate embryonic stem cells with helper-dependent adenoviral vectors. Proc. Natl. Acad. Sci. U. S. A. 105, 13781–13786.

Takahashi, K., Yamanaka, S., 2006. Induction of pluripotent stem cells from mouse embryonic and adult fibroblast cultures by defined factors. Cell 126, 663–676.

Takahashi, K., Tanabe, K., Ohnuki, M., Narita, M., Ichisaka, T., Tomoda, K., Yamanaka, S., 2007. Induction of pluripotent stem cells from adult human fibroblasts by defined factors. Cell 131, 861–872.

Takahashi, K., Narita, M., Yokura, M., Ichisaka, T., Yamanaka, S., 2009. Human induced pluripotent stem cells on autologous feeders. PLoS One 4, e8067.

Thomas, K.R., Capecchi, M.R., 1987. Site-directed mutagenesis by gene targeting in mouse embryo-derived stem cells. Cell 51, 503–512.

Thomson, J.A., Itskovitz, Eldor J., Shapiro, S.S., Waknitz, M.A., Swiergiel, J.J., Marshall, V.S., Jones, J.M., 1998. Embryonic stem cell lines derived from human blastocysts. Science 282, 1145–1147.

Torre, C., Perret, C., Colnot, S., 2011. Transcription dynamics in a physiological process: beta-catenin signaling directs liver metabolic zonation. Int. J. Biochem. Cell Biol. 43, 271–278.

Touboul, T., Hannan, N.R., Corbineau, S., Martinez, A., Martinet, C., Branchereau, S., Mainot, S., Strick, Marchand H., Pedersen, R., Di, Santo J., Weber, A., Vallier, L., 2010. Generation of functional hepatocytes from human embryonic stem cells under

chemically defined conditions that recapitulate liver development. Hepatology 51, 1754–1765.

Umana, P., Gerdes, C.A., Stone, D., Davis, J.R., Ward, D., Castro, M.G., Lowenstein, P.R., 2001. Efficient FLPe recombinase enables scalable production of helper-dependent adenoviral vectors with negligible helper-virus contamination. Nat. Biotechnol. 19, 582–585.

Urbach, A., Schuldiner, M., Benvenisty, N., 2004. Modeling for Lesch-Nyhan disease by gene targeting in human embryonic stem cells. Stem Cells 22, 635–641.

Zaret, K.S., Grompe, M., 2008. Generation and regeneration of cells of the liver and pancreas. Science 322, 1490–1494.

Zou, J., Maeder, M.L., Mali, P., Pruett, Miller S.M., Thibodeau, Beganny S., Chou, B.K., Chen, G., Ye, Z., Park, I.H., Daley, G.Q., Porteus, M.H., Joung, J.K., Cheng, L., 2009. Gene targeting of a disease-related gene in human induced pluripotent stem and embryonic stem cells. Cell Stem Cell 5, 97–110.

Zwaka, T.P., Thomson, J.A., 2003. Homologous recombination in human embryonic stem cells. Nat. Biotechnol. 21, 319–321.